DEMONSTRATION OF TISSUE ALTERATIONS BY ULTRASONOGRAPHY, MAGNETIC RESONANCE IMAGING AND SPECTROSCOPY, AND HISTOLOGY IN BREAST CANCER PATIENTS WITHOUT LYMPHEDEMA AFTER AXILLARY NODE DISSECTION

A. Tassenoy, K. Vermeiren, P. van der Veen, T. Stadnik, F. De Ridder,
E. Peeters, P. Van Schuerbeek, J. Lamote, P. Lievens

Departments of Rehabilitation Research (AT,KV,PVDV,PL), Radiology (TS,FDR,PVS), and Thoracic Surgery (JL), Vrije Universiteit Brussel, Brussels, Belgium

ABSTRACT

Estimates of the incidence of arm swelling after axillary lymph node dissection for breast cancer range from 10 to 37%. Yet the subjective sensation of edema is described in at least 54% of patients. The purpose of this research was to examine the structural changes occurring in the subcutaneous tissue that might explain these subjective complaints using multiple imaging modalities. Two female cadavers with unilateral breast amputation and axillary dissection were studied. The dermal and subcutaneous layers of both arms were visualized with high frequency ultrasonography, and magnetic resonance imaging and spectroscopy (MRS), and tissue biopsies were taken for histological evaluation.

On the operated side, ultrasound imaging showed a hyperechogenic subcutis and the fat-to-water relationship in adipose cells was higher as measured by MRS. Dissection of the arms revealed structural adipose tissue changes, which were confirmed by microscopic evaluation.

Keywords: breast cancer, lymphedema, ultrasound imaging, magnetic resonance imaging, nuclear magnetic resonance spectroscopy, soft tissue histology, adipogenesis

Lymphedema is the most common and significant complication after axillary lymph node dissection for breast cancer treatment. The incidence of swelling has been reported in a wide range from 10% to 37%, due to use of different measurement techniques and varying definitions of swelling.

Patients without a clinically evident or objectively measurable increase of arm volume not uncommonly have a subjective sensation of arm swelling (1). A study of Schrenk et al (2) reported that 54% of patients with axillary lymph node dissection report a mild to moderate sensation of arm swelling. Kuehn et al (3) found a discrepancy between the self-reported symptom intensity for edema and the objective findings on physical examination. This degree of intensity was classified as more severe by patients themselves than would have been suggested by the results of clinical examination. In prior studies by van der Veen et al (4,5) concerned with the incidence of edema, 44.9% of the patients complained of subjective edema, of whom 53.5% had no objectively measurable edema.

The aim of this study was to investigate whether structural changes in the soft tissues occur in patients with axillary lymph node dissection without overt edema as an

Fig. 1. MRI setting: arms are positioned in a phased array coil for imaging using the 1.5T Symphony MR system.

Fig. 2. Photographic display of the locations for tissue biopsies taken of the arm.

explanation for this subjective feeling of arm swelling. Ultrasonography, magnetic resonance imaging and spectroscopy were used for visualization of the tissues and images were compared with microscopic findings from tissue biopsies.

SUBJECTS, MATERIALS, AND METHODS

For the imaging studies and histologic examination of tissue, two human cadavers with unilateral breast amputation and axillary lymph node dissection were studied. There was no visual difference in arm volumes suggesting post-operative arm edema. In one cadaver, circumferences were measured at 4 cm intervals from wrist to axilla and arm volume calculated from the truncated cone formula, and a small 8% greater volume (116 ml) was recorded on the operated compared to non-operated side.

The different levels for imaging and tissue biopsy were marked on the arms.

Ultrasound Imaging

Dual images were obtained using a Siemens ultrasound system with an 11 MHz transducer. Images on the anterior side of the arm were taken transversely to the length axis of the arm. Field size was set to 256 mm wide and 128 mm depth. A two-dimensional

image was produced, recorded by computer, and viewed in gray scale.

The thickness of the dermis and the sub-cutis was determined by measuring between the entry echo and the dermis/subcutis boundary for skin thickness and between the bottom of the dermis and the line generated by the fascial connective tissue sheet overlying the muscle for subcutis.

Magnetic Resonance (MR) Imaging and Spectroscopy

MR imaging and spectroscopy were carried out using a 1.5T Symphony MR system (Siemens, Erlangen, Germany) (Fig. 1). Both arms were positioned in a phased array coil (12 segments) with the body in a supine position. Vitamin A pearls were attached to the skin with adhesive tape on 6 levels as markers.

Two-dimensional T2 axial and transverse images (Turbo Spin Echo) were generated with time of repetition (TR) = 3910 ms, time of echo (TE) = 104 ms and flip angle (FLα) of 90°. The field of view (FOV) was 160 X 160 mm, the matrix (Ma) 224 X 320 mm and the thickness of a slice 3 mm. T1 TSE settings were TR = 884 ms, TE = 12 ms, FLα of 180°, FOV = 120 X 120 mm, Ma = 180 X 320 mm and slice thickness 3 mm. MP-RAGE (Magnetization-Prepared Rapid-acquired

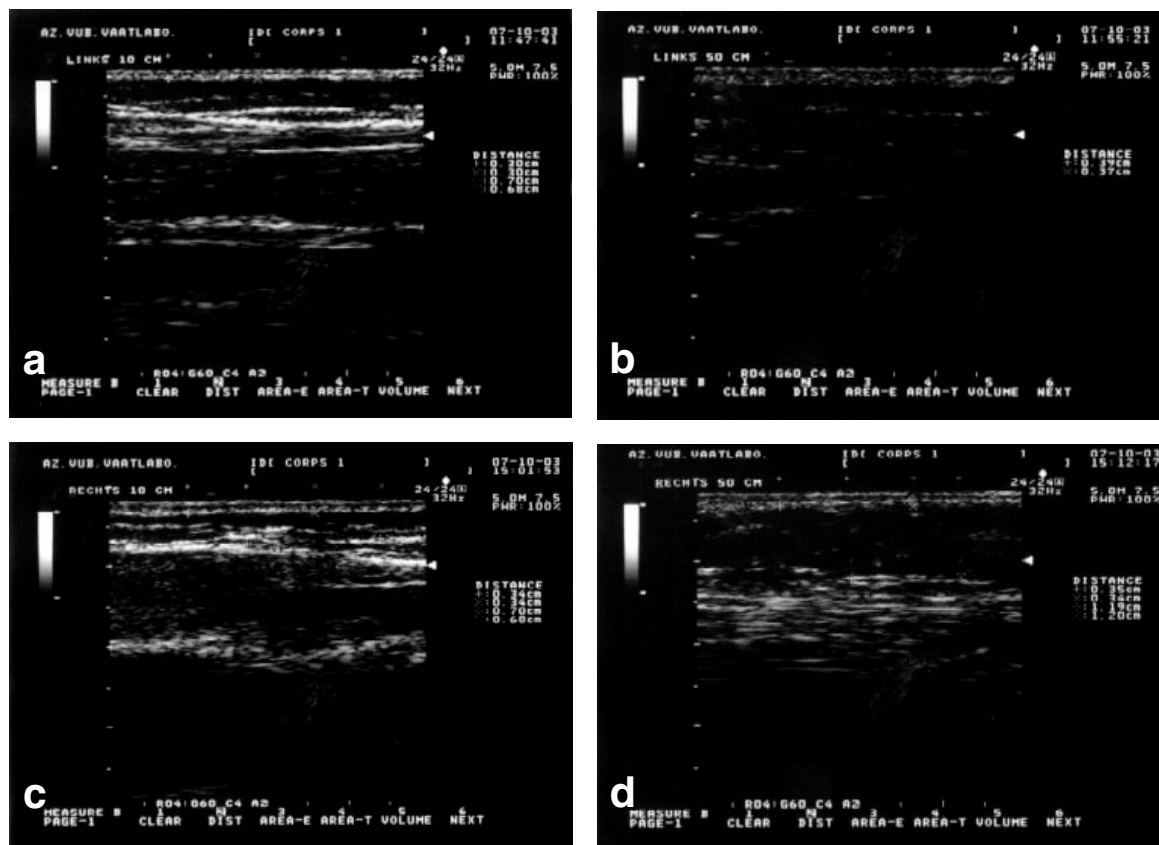| TABLE 1		
Mean Thickness of the Dermis and Subcutis of Both Cadavers		
	Thickness	
	Operated side	Non-operated side
Mean dermis	0.67 mm	0.65 mm
Mean subcutis upper arm	9.0 mm	8.62 mm
Mean subcutis forearm	5.57 mm	6.25 mm

Fig. 3. Ultrasonographic images of the upper (a) and forearm (b) on the non-operated side and of the upper (c) and forearm (d) on the operated side. Note a hyperechogenic subcutis on the operated side.

gradient echo) 3D images were obtained with TR = 2000 ms, TE = 4.3 ms, FLα = 12°, FOV = 160 X 160, Ma = 256 X 256, and slice thickness 2 mm. FLAIR (Fluid Attenuated Inversion Recovery) images were obtained with TR = 9000 ms, TE = 110 ms, FLα = 180°, FOV = 450 X 450, Ma = 512 X 256, and slice thickness 8 mm.

TABLE 2
Amount of Fatty Acids Related to Water Content Measured by MRS

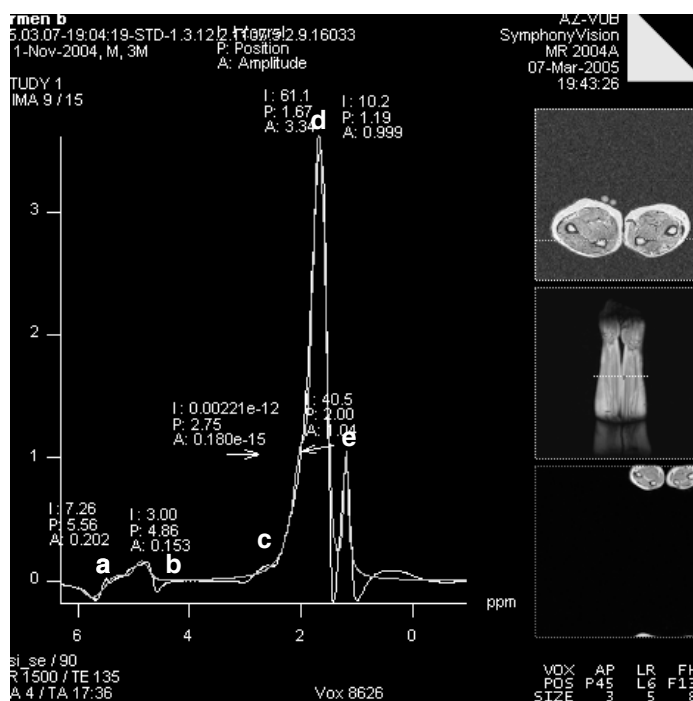| F/W	Operated side	Non-operated side
CH=CH (a)	3.01	1.43
-CH3 (c)	4.97	4.86
(CH2)n (d)	22.58	18.46
-CH=CH-CH2 (e)	13.64	7.35
Mean Fatty Acids/Water	44.20	32.10

Fig. 4. Example of MRS of the subcutaneous tissue showing different peaks of fatty acids (a, c, d & e, see Table 2) and water (b) in the non-operated arm.

Diffusion weighted echo planar images were included in the MRI evaluation because this sequence is very sensitive to cytotoxic edema (increased water content in cells). In order to get information about water and fat distribution in lymphedema, a chemical shift imaging sequence was applied. Images were acquired with a TR of 1500 ms and TE of 135 ms. The voxel size was 3 x 5 x 8 mm^3 and was situated in the subcutaneous layer in the middle of the forearm.

Tissue Histology

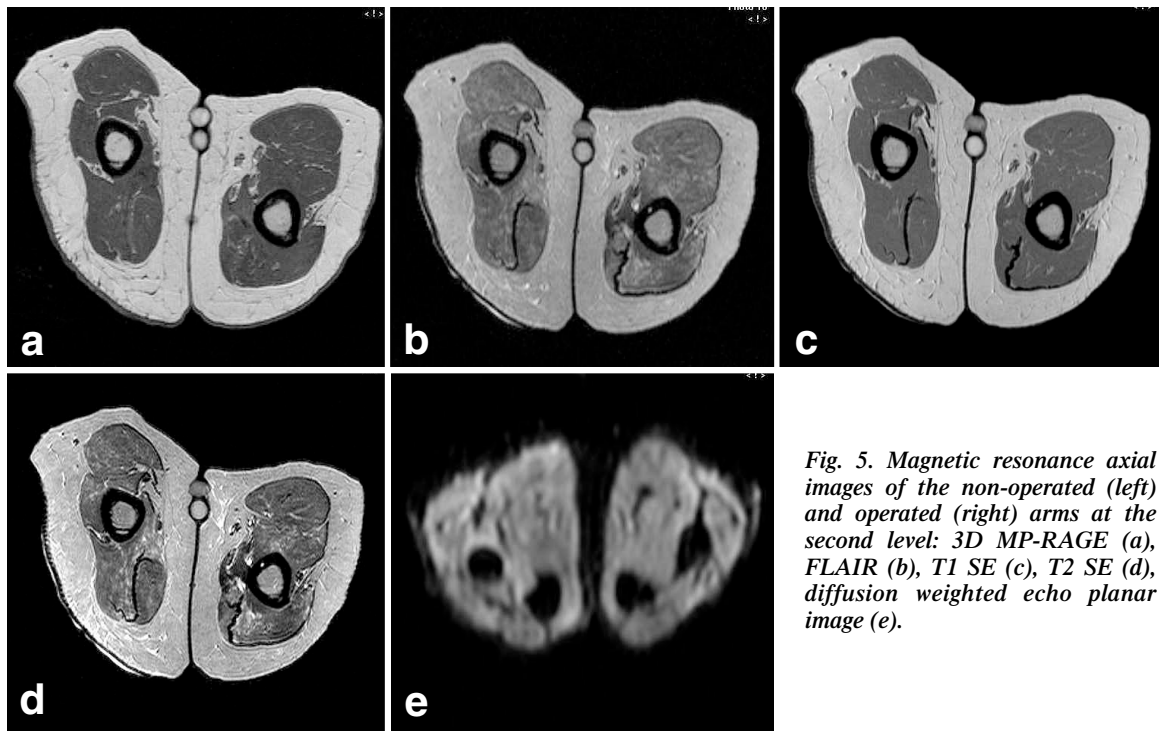Tissue biopsies were taken at the different levels of imaging. Incisions were

Fig. 5. Magnetic resonance axial images of the non-operated (left) and operated (right) arms at the second level: 3D MP-RAGE (a), FLAIR (b), T1 SE (c), T2 SE (d), diffusion weighted echo planar image (e).
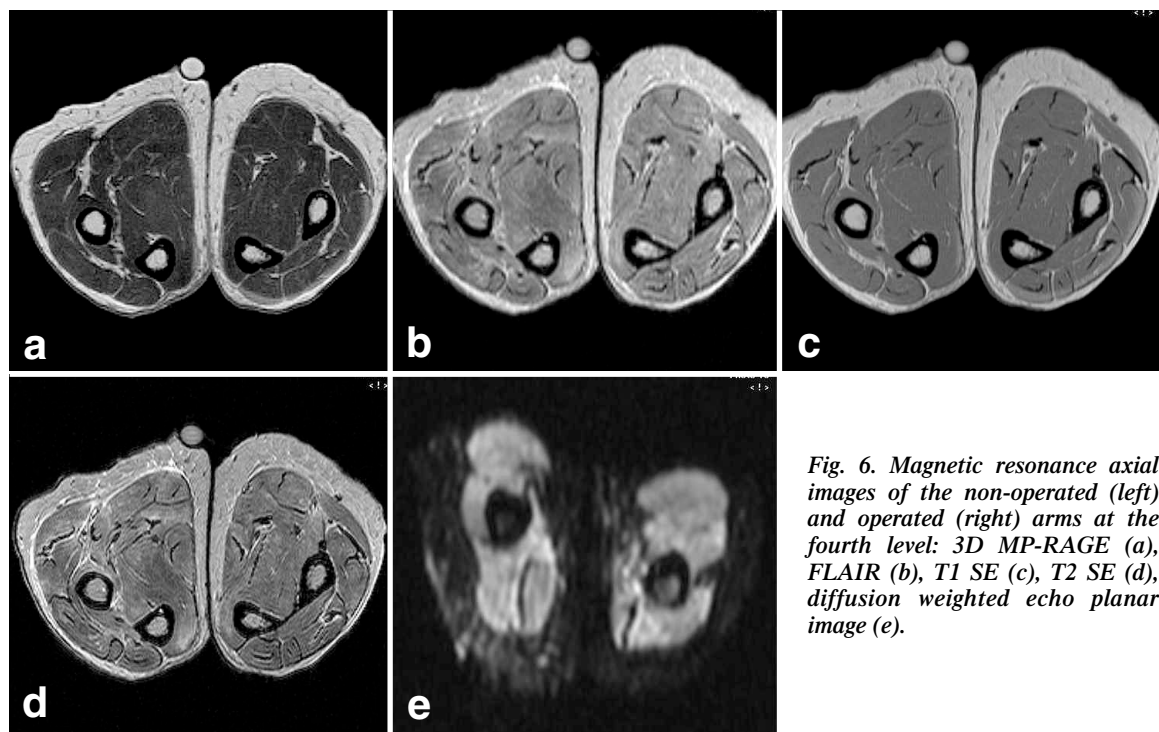

Fig. 6. Magnetic resonance axial images of the non-operated (left) and operated (right) arms at the fourth level: 3D MP-RAGE (a), FLAIR (b), T1 SE (c), T2 SE (d), diffusion weighted echo planar image (e).
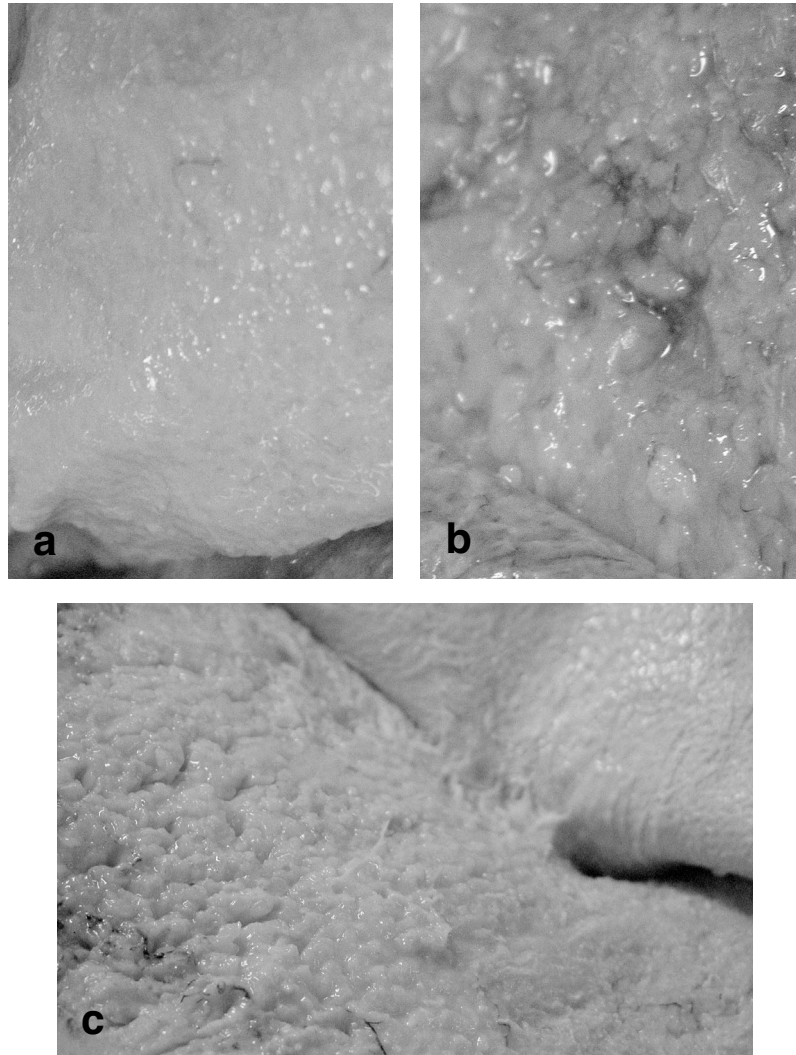
Fig. 7. Gross morphological structure of the arm displaying differences in fat presentation on the non-operated (a) and operated side (b). Note also fibrotic adhesions seen on the operative side (c).

made up to the level of the muscle fascia *(Fig. 2)*. Tissues were formaldehyde fixed and embedded in paraffin. Slices were stained with Haematoxylin-Eosin for a general tissue picture and with Masson Trichrome for collagen visualization. This latter technique stains nuclei blue-black, cytoplasm, muscle cells and erythrocytes red, and collagen blue. Microscopic images were recorded by computer and viewed in Adobe Photoshop®. The ImageJ program (National Institutes of Health, Bethesda, MD, http://rsb.info.nih.gov/ij/) was used to determine the cell area by calculating the surface of a selected area after setting the picture scale.

RESULTS

Ultrasound Imaging

Dermal and subcutaneous thickening of the operated arm was minimal for both
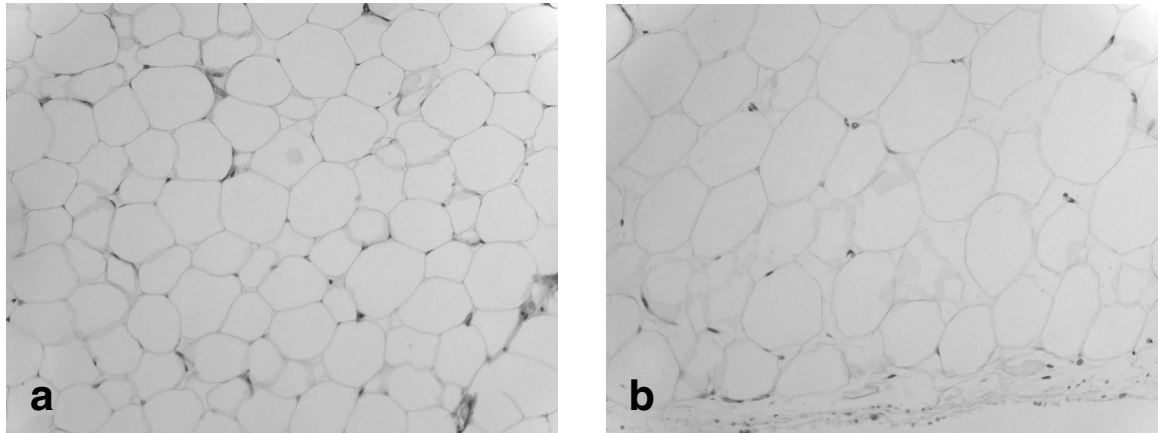
Fig. 8. Microscopic images of adipose cells from the non-operated (a) and operated side (b) showing larger cells less densely packed on the operated side.

cadavers. *Table 1* summarizes thickness measurements of the different layers.

Images depicted a hyperechogenic dermis and a hypoechogenic subcutis on the healthy side. The subcutaneous layer on the operated side was more hyperechogenic than on the healthy side. Most changes were in the portion of the subcutis near the muscle fascia *(Fig. 3)*. Few dermal changes are seen.

Magnetic Resonance Imaging and Spectroscopy

The spectra depicted different peaks, representing water, saturated and unsaturated fat molecules *(Fig. 4)*. The relative amount of fat in the subcutis was calculated by dividing the area under the water peak by the area under the fat peaks *(Table 2)*. The highest values were shown on the healthy side but relatively more (un)saturated fat molecules were found on the operated side.

Figures 5 and 6 show axial slices of the second and fourth level 3D MP-Rage (a), FLAIR (b), T1 weighted spin echo (c), T2 weighted spin echo (d), diffusion weighted echo planar imaging (DW EPI) (e).

On the sequences performed, including DW EPI, there was no clear difference in the signal intensity or morphological evaluation that would suggest increased water content (edema) or fibrosis in the subcutaneous layer. No difference in muscle mass was seen.

Tissue Histology

Macroscopically, skin dissection of the arms revealed a more granular pattern of the subcutaneous fat tissue *(Fig. 7a,b)* and fibrotic adhesions *(Fig. 7c)* to the dermal layer in the operated arm.

Microscopically, the surface areas of adipose cells determined using the ImageJ program showed that the operated side cells were significantly (p<0.001) larger and less densely packed per unit area than on the healthy side by an average of 50% *(Fig. 8)*.

Masson Trichrome staining demonstrated collagen fibers in fibrotic bands within the adipose tissue on both the operated side and non-operated side.

DISCUSSION

Many studies have reported the presence of subjective feelings of arm swelling in patients following axillary lymph node dissection. We studied two female human cadavers with unilateral mastectomy and axillary lymph node dissection and without objectively measurable edema of the upper limb. Despite

the absence of arm swelling, imaging procedures and tissue histological examination revealed some structural tissue changes.

Ultrasound imaging showed a hyperechogenic subcutis, but no increased thickness of the dermal and subcutaneous layer and the fat-to-water ratio in the subcutaneous layer was higher on the operated side as measured by MRS. Tissue dissection revealed structural adipose tissue changes, which were confirmed by microscopic evaluation.

In cases of advanced lymphedema, ultrasonographic investigation (6-8) of lymphedematous tissue has shown a significant increase in the skin and subcutis thickness. Dimakakos et al (7) described a stone-pave picture: irregular subcutaneous areas of increased echogenicity surrounded by thin non-echogenic bands. This was attributed to intracellular fluid. Doldi et al (8) interpreted the hypoechogenic subcutis layer as fibrosclerosis. In the present study, only a slight change in echogenicity was observed. The edema had not evolved to an advanced stage where this typical stone pave picture can be seen.

MRI studies have confirmed this thickening of both layers in cases of edema (7,9-11). An increase of fat and adipogenesis is also mentioned by Idy-Peretti et al (12) and Case et al (11). A subcutaneous honeycomb pattern has been reported by different authors, with a variety of explanations about the composition of this structure. Astrom et al (13) describe it as an excess of interstitial fluid between areas of fat lobules, free in hydraulic chambers or trapped in collagen tissue and hyaluronic acid molecules. Case et al (11) and Fujii (9) also mention fat pockets but surrounded by a trabeculum of fibrotic or fluid-filled dilated lymph vessels. Dimakakos et al (7) and Haaverstad et al (10) interpret the finding as accumulated fat surrounded by fibrotic tissue and fluid. Werner et al (14) describe them as deep hydraulic chambers separated by collagen fibers. In this cadaveric study, no similar structural alternations were observed with magnetic resonance imaging.

CONCLUSION

Despite absence of significant objectively measurable arm swelling, subcutaneous tissue changes take place in some patients as seen in this cadaveric study. These changes might explain why in more than half of the axillary lymph node dissections, patients complain of subjective feelings of arm swelling. These findings support the importance of a preventive role for components of complex physical therapy in patients without objectively measurable edema after breast cancer treatment in order to avoid or minimize these ongoing structural tissue changes related to sub-clinical lymphatic dysfunction.

ACKNOWLEDGMENT

REFERENCES

1. Borup Christensen, S, E Lundgren: Sequelae of axillary dissection vs. axillary sampling with or without irradiation for breast cancer. A randomized trial. Acta Chir. Scand. 155 (1989), 515-519.
2. Schrenk, P, R Rieger, A Shamiyeh, et al: Morbidity following sentinel lymph node biopsy versus axillary lymph node dissection for patients with breast carcinoma. Cancer 88 (2000), 608-614.
3. Kuehn, T, W Klauss, M Darsow, et al: Long-term morbidity following axillary dissection in breast cancer patients-clinical assessment, significance for life quality and the impact of demographic, oncologic and therapeutic factors. Breast Cancer Res. Treat. 64 (2000), 275-286.
4. van der Veen, P, K Vermeiren, K Von Kemp, et al: A key to understanding postoperative lymphoedema: a study on the evolution and consistency of oedema of the arm using ultrasound imaging. Breast 10 (2001), 225-230.
5. van der Veen, P, N De Voogdt, P Lievens, et al: Lymphedema development following

breast cancer surgery with full axillary resection. Lymphology 37 (2004), 206-28.

6. Mellor, RH, NL Bush, AW Stanton, et al: Dual-frequency ultrasound examination of skin and subcutis thickness in breast cancer-related lymphedema. Breast J. 10 (2004), 496-503.

7. Dimakakos, PB, T Stefanopoulos, P Antoniades, et al: MRI and ultrasonographic findings in the investigation of lymphedema and lipedema. Intl. Surg. 82 (1997), 411-416.

8. Doldi, SB, E Lattuada, MA Zappa, et al: Ultrasonography of extremity lymphedema. Lymphology 25 (1992), 129-133.

9. Fujii, K: MR imaging of edematous limbs in lymphatic and nonlymphatic edema. Acta Radiol. 35 (1994). 262-269.

10. Haaverstad, R, G Nilsen, PA Rinck, et al: The use of MRI in the diagnosis of chronic lymphedema of the lower extremity. Intl. Angiol. 13 (1994), 115-118.

11. Case, TC, CL Witte, MH Witte, et al: Magnetic resonance imaging in human lymphedema: Comparison with lymphangio-scintigraphy. Mag. Res. Imaging 10 (1992), 549-558.

12. Idy-Peretti, I, J Bittoun, FA Alliot, et al: Lymphedematous skin and subcutis: In vivo high resolution magnetic resonance imaging evaluation. J. Invest. Dermatol. 110 (1998), 782-787.

13. Astrom, KG, S Abdsaleh, GC Brenning, et al: MR imaging of primary, secondary, and mixed forms of lymphedema. Acta Radiol. 42 (2001), 409-416.

14. Werner, GT, R Scheck, E Kaiserling: MR of edematous limbs. Acta Radiologica 37 (1996), 972-973.

Dr. A. Tassenoy
Vrije Universiteit Brussel
Department of Rehabilitation Research
Laarbeeklaan 103
1090 Brussel, Belgium
Telephone: 0032 2 477 45 30
Fax: 0032 2 477 45 29
E-mail: antassen@vub.ac.be